DOI: 10.1002/chem.200701605

Templated Synthesis of Electroactive Periodic Mesoporous Organosilica Bridged with Oligoaniline

Yi Guo,[a] Andreas Mylonakis,[a] Zongtao Zhang,[a, d] Guoliang Yang,[b] Peter I. Lelkes,[c] Shunai Che,[e] Qinghua Lu,[e] and Yen Wei*[a]

Abstract: The synthesis and characterization of novel electroactive periodic mesoporous organosilica (PMO) are reported. The silsesquioxane precursor, *N,N′*-bis(4′-(3-triethoxysilylpropylureido)phenyl)-1,4-quinonene-diimine (TSUPQD), was prepared from the emeraldine base of amino-capped aniline trimer (EBAT) using a one-step coupling reaction and was used as an organic silicon source in the co-condensation with tetraethyl orthosilicate (TEOS) in proper ratios. By means of a hydrothermal sol–gel approach with the cationic surfactant cetyltrimethylammonium bromide (CTAB) as the structure-directing template and acetone as the co-solvent for the dissolution of TSUPQD, a series of novel MCM-41 type siliceous materials (TSU-PMOs) were successfully prepared under mild alkaline conditions. The resultant mesoporous organosilica were characterized by Fourier transform infrared (FT-IR) spectroscopy, thermogravimetry, X-ray diffraction, nitrogen sorption, and transmission electron microscopy (TEM) and showed that this series of TSU-PMOs exhibited hexagonally patterned mesostructures with pore diameters of 2.1–2.8 nm. Although the structural regularity and pore parameters gradually deteriorated with increasing loading of organic bridges, the electrochemical behavior of TSU-PMOs monitored by cyclic voltammetry demonstrated greater electroactivities for samples with higher concentration of the incorporated TSU units.

Keywords: conducting materials · electrochemistry · mesoporous materials · periodic mesoporous organosilica · sol–gel processes

Introduction

Since MCM-41 type periodic mesoporous silica was first introduced in 1992 using a lyotropic surfactant templating route,[1] a considerable amount of work has been conducted in exploring functional hybrid materials based on this new type of silica, which host organic or biological guests in hexagonal-patterned void frameworks.[2] In recent years, periodic mesoporous organosilica (PMO) was discovered and has attracted increasing attention.[3] In general, this innovative class of hybrid materials are synthesized from hydrolysis and co-condensation of bridged silsesquioxanes $(RO)_3Si\text{-}R'\text{-}Si(OR)_3$ and tetraethyl orthosilicate (TEOS) by using a surfactant-mediated self-assembly method.[4] A huge diversity of cationic, anionic, and nonionic surfactants has been employed to afford different two-dimensional and three-dimensional structures including hexagonal and cagelike cubic structures[5] with uniformly distributed functionality in the silica framework, while retaining structural rigidity and well-ordered mesopores.[6] PMOs exhibit distinct properties over conventional mesoporous silica and other hybrid materials, such as enhanced flexibility, "crystalline" pore walls,[7] tuna-

[a] Dr. Y. Guo, A. Mylonakis, Prof. Z. Zhang, Prof. Y. Wei
Department of Chemistry, Drexel University
Philadelphia, Pennsylvania 19104 (USA)
Fax (+1) 215-895-1265
E-mail: weiyen@drexel.edu

[b] Prof. G. Yang
Department of Physics, Drexel University
Philadelphia, PA 19104 (USA)

[c] Prof. P. I. Lelkes
School of Biomedical Engineering & Engineering
Drexel University, Philadelphia, PA 19104 (USA)

[d] Prof. Z. Zhang
Department of Chemistry, Jilin University
Changchun 130023 (China)

[e] Prof. S. Che, Prof. Q. Lu
School of Chemistry & Chemical Technology
Shanghai Jiao Tong University, Shanghai, 200030 (China)

Supporting information for this article is available on the WWW under http://www.chemeurj.org/ or from the author.

ble hydrophilicity/hydrophobicity,[8] magnetic,[9] and optical[10] properties.

The integrated organic bridges in PMOs are mainly limited to short aliphatic, aromatic, or organometallic building units,[3,12a–d] which are more favorable in balancing the kinetics and interfacial thermodynamics than larger organic groups during the process of organosilica formation.[11] This limitation strictly hinders PMOs from a broader range of applications.[12] To expand the diversity of PMOs for different applications, new bridging groups need to be introduced into the silica framework while retaining the desired physical properties of siliceous materials. For example, in electrocatalytic applications, multi-functionality, as well as deliberate disorders, are essential to provide facile and rapid heterogeneous catalysis for small molecules.[13] For the purpose of making sensor devices, a combination of high surface area and electronic conductivity is required for enhanced electric response.[14] However, only a few successful studies on synthesizing novel PMOs with large bridging groups and multifunctionality have been reported.[15] Kuroki et al. synthesized a 1,3,5-benzene PMO showing unique thermal transformations.[16] Liu et al. incorporated thioether groups into the MCM-41 silica framework and obtained increased hydrothermal stability and large adsorption ability towards Hg^{2+} and phenol.[17] Grudzien et al. synthesized the bifunctional PMOs with a combination of "flexible" ethane and "bulky" isocyanurate bridging groups.[18]

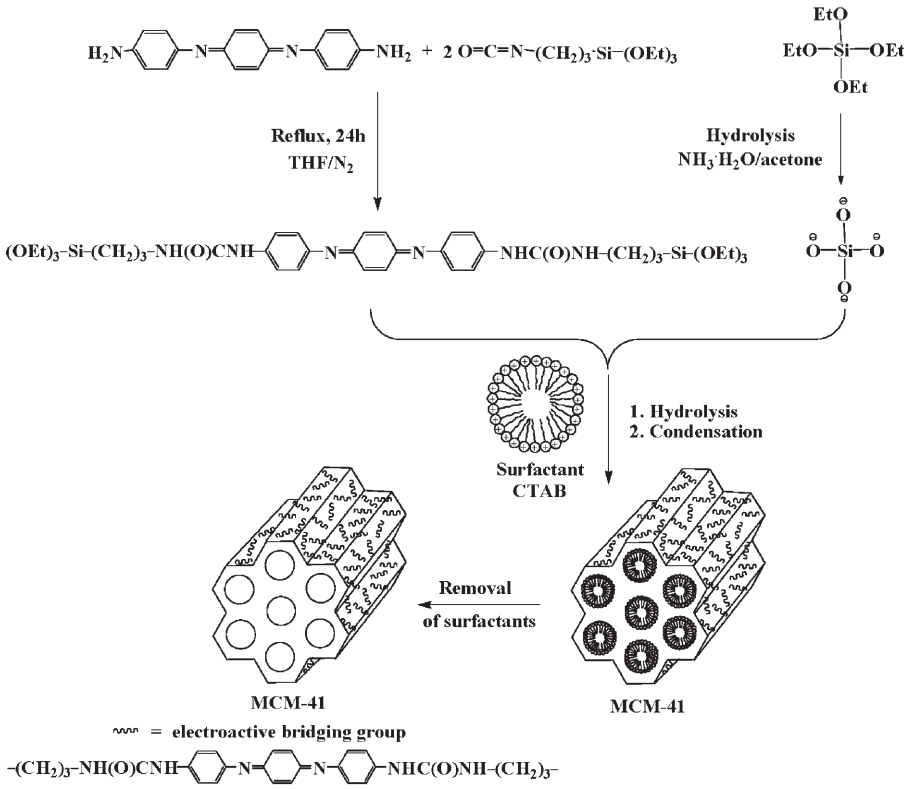

Scheme 1. Synthesis of electroactive TSU-PMO.

In preparing electroactive hybrid materials, electrochemically active guests such as polyoxometalate,[19] ferrocenyl[20] groups, and enzyme glucose oxidase[21] have been grafted into the mesoporous silica matrix. Comparatively, electroactive PMOs made by co-condensation have advantages over these post-synthetically functionalized materials in that the electroactive organic moieties are homogeneously distributed in the inorganic matrix without severely occupying the inner void space.[6] Herein, we report the successful synthesis of a series of novel electroactive periodic mesoporous organosilica with amino-capped aniline trimer units as bridges. Aniline trimer was chosen because it exhibits similar intrinsic physical properties and electroactive behavior to polyaniline[22] due to the same oxidation and protonic doping mechanisms (Scheme 1). The silsesquioxane compound *N,N′*-bis-(4′-(3-triethoxysilylpropylureido)phenyl)-1,4-quinonene-diimine (TSUPQD) was synthesized from the emeraldine base of an aniline trimer[23] and was used as the precursor which underwent hydrolysis and co-condensation with TEOS in a cetyltrimethylammonium bromide (CTAB) templating hydrothermal sol-gel method using acetone as the co-solvent. Removal of CATB surfactants from the hexagonally ordered oligoaniline-containing silica afforded the novel electroactive periodic mesoporous organosilica (TSU-PMOs) which had high surface areas and contained uniformly distributed electroactive units inside the pores. Possessing both incorporated tunable electroactivity and surface charges, TSU-PMOs can be potential candidates as switchable host-guest systems for delivering bioactive molecules, such as drug molecules, proteins, and DNA. They are also promising as future electrocatalysts and biosensor electrodes with enhanced performance.

Results and Discussion

As illustrated in Scheme 1, an emeraldine-base aniline trimer was allowed to react with triethoxysilylpropyl isocyanate (TESPIC) to give the electroactive silsesquioxane precursor TSUPQD, which was then incorporated into the silica matrix using hydrolysis and co-condensation with TEOS with CTAB as the structure template. To successfully assemble organosilica into a periodic mesophase, appropriate template-precursor interfacial energy must be employed.

Favorable interfacial energy such as hydrophilic–hydrophobic interactions and electrostatic forces can help the PMO formation, even with sterically hindered organic bridges. Hydrophilic–hydrophobic interactions are crucial in controlling the formation of micelles while charge matching (S^+I^-) between the surfactant head group and the silanolate ($Si–O^-$) effects the molecular structure. Factors in tuning the template-precursor interfacial energy include temperature, concentration, pH value, co-surfactant, co-solvent, and incorporation of organic additives.[25] In our synthesis of TSU-PMOs, the precursor TSUPQD was condensed at room temperature under mild basic condition (pH ≈8–9) with cationic CTAB as the template. The basic environment kept TSUPQD in the emeraldine-base form which eliminated the electrostatic interference from the positively charged aniline trimer unit and was much easier to process in organic solvents[26] than the doped-salt. Acetone was used as a co-solvent to help dissolve TSUPQD without any significant influence on the assembling of precursors and surfactant micelles into ordered mesophase structures, as proved by XRD and nitrogen sorption measurements.

The presence of oligoaniline units in the TSU-PMOs was proven by IR spectroscopy (Figure 1). The strong bands at

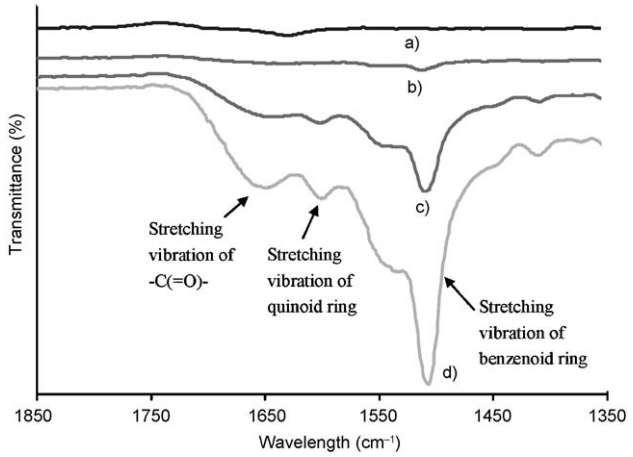

Figure 1. FT-IR spectra of surfactant-free TSU-PMOs. a) 0 wt% TSU-PMO; b) 10 wt%; c) 33 wt%; d) 66 wt%.

1500 cm^{-1}–1700 cm^{-1} are characteristic of oligoaniline groups. Two sharp bands at 1500 and 1600 cm^{-1} are attributed to stretching vibrations of the benzenoid and quinoid groups, respectively.[27] The much stronger benzenoid absorption compared to the quinoid band confirmed that, after acid-extraction, the surfactant-free samples are an emeraldine salt. The weak band at 1650 cm^{-1} is associated with C=O stretching in the ureido unit. Two small peaks at 2860 and 2920 cm^{-1} (see Figure S1 in the Supporting Information), corresponding to saturated C–H bond stretching absorption, are assigned to the $-(CH_2)_3-$ unit in the TSUPQD precursor. All of the synthesized TSU-PMOs show very similar IR spectra with differences only in the relative band intensities. Increasing amounts of TSUPQD used during the synthesis leads to increased absorption intensity. As shown in Figure 1, the discernible peaks (1500, 1600, 1650 cm^{-1}) for 66 wt% TSU-PMO (Figure 1d) gradually attenuate with decreased organic contents in TSU-PMOs (Figure 1c–a).

To investigate the thermal stability of the oligoaniline moieties in the silica mesostructure, thermogravimetric analyses (TGA) were conducted (from room temperature to 800°C in air) for both the TSU-PMOs and the hybrids before removal of surfactant. As shown in Figure 2 A and B,

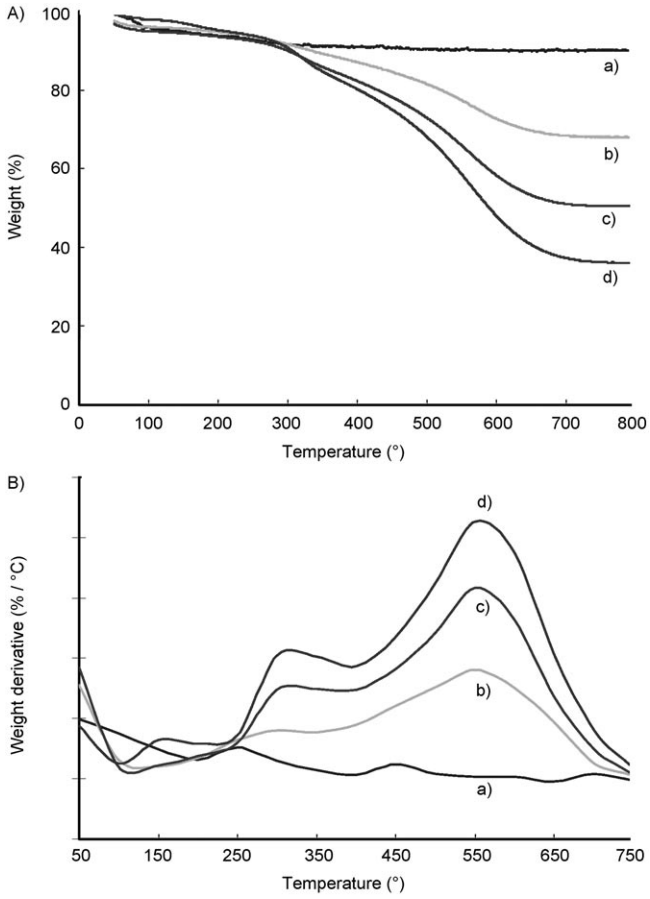

Figure 2. Thermogravimetric plots (A) and derivative weight loss curves (B) after surfactant extraction. a) 0 wt% TSU-PMO, b) 20 wt%, c) 33 wt%, d) 66 wt%.

TSU-PMOs with different loading of oligoaniline bridging groups exhibit different TGA profiles and corresponding derivative weight loss curves (DTG). Increasing the concentration of organic groups leads to higher peak intensities in the DTG curves, but does not affect the pattern of the thermal decomposition. The TGA curves of the hybrid materials before surfactant extraction (see Figure S2 in the Supporting Information) show remarkable weight losses (10–26 wt%) at about 255°C due to the thermal degradation of the surfactant CTAB. It is worth noting that 5 wt% TSU-PMO showed the highest weight loss in this temperature region, implying the highest amount of surfactant encapsulated in the matrix, which indicates the largest pore volume and sur-

face area in this composite. In profiles of the template-free organosilica (Figure 2), the 1–2 wt% weight losses below 100 °C resulted from residual ethanol and physisorbed moisture. The major decomposition peaks at about 550 °C on the DTG curves correspond to the oligoaniline units which agreed with our previous study,[23] in that the aniline trimer appears to be stable up to 400 °C. The minor decomposition peaks between 250 °C and 400 °C are assigned to ureidopropyl groups. Moreover, the weights of the residues which survived after 800 °C are in good agreement with the theoretical values calculated stoichiometrically. (Table 1) For example, in 20 wt% TSU-PMO, the sample yielded 68.9% SiO_2 at 800 °C which is consistent with the theoretical value of 69.1% SiO_2. This agreement further confirms the complete extraction of surfactants by the hydrochloric acid–ethanol mixture.

Table 1. Concentration of bridging groups in the TSU-PMOs.

TSUPQD:TEOS ratio [wt%/wt%]	Mass used as precursor		Bridging group/ SiO_2 [wt%]	Bridging group in the TSU-PMO product [wt%]
	TSUPQD [mg]	TEOS [mg]		
0:100	0	200	0	0
5:95	10	190	10.4	9.42
10:90	20	180	21.2	17.49
20:80	40	160	44.7	30.89
33:67	80	160	79.0	44.13
66:34	160	80	193.5	65.93
100:0	200	0	381.0	79.21

Small angle XRD diagrams of TSU-PMOs (Figure 3) show that the materials with appropriate loading of oligoaniline bridges retain the two dimensional hexagonal crystallographic structure resembling typical MCM-41 pattern,[1] with three low-angle Bragg diffraction peaks indexed as the (100), (110), and (200) reflection planes of the hexagonal space group *P6mm*.[7] While the oligoaniline concentration increases, the 2θ angle increases, indicating a decrease of interlayer spacing. Meanwhile, peak intensities gradually attenuate, reflecting deteriorating structural ordering of the silica framework. For example, for 66 wt% TSU-PMO, d-spacing reduces from 4.0 nm (5 wt% TSU-PMO) to 3.8 nm, the (100) peak is notably broadened and the higher order (110) and (200) reflections disappear, which suggest a lower structural regularity of the silica matrix. Broadening and darkening of the Debye–Scherrer diffraction pattern (Figure 3 inserts) further confirms the decreased structural order associated with increased oligoaniline content. These changes in X-ray diffraction profiles parallel other functionalized PMOs previously reported.[28] The d_{100} spacings and calculated inter-pore distances a_0 for several representative TSU-PMOs materials are listed in Table 2. Wide-angle XRD measurements (see Figure S3 A-B in the Supporting Information) were used to examine the effect of co-condensation of TSUPQD and TEOS, which show a broad amorphous band of TSU-PMOs centered at $2\theta \approx 21°$. By contrast, wide-angle XRD measurements were also conducted on physical mixtures of two type silica materials at a series of weight ratios, one from self-condensation of TSUPQD and the other from self-condensation of TEOS. Their XRD profiles show different patterns to those of TSU-PMOs. They feature a broad amorphous domain with a group of inner rings superimposed on top from $2\theta \approx 6°$ to $2\theta \approx 25°$. These crystalline peaks resemble those of the emeraldine base (EB) polyaniline and arise from the ordered patterning of oligoaniline moieties.[23] These results strengthened the notion that the combination of TEOS and the bis-silylated TSUPQD afforded homogeneous sols in the course of co-condensation and eventually led to homogeneous hybrid materials TSU-PMOs.

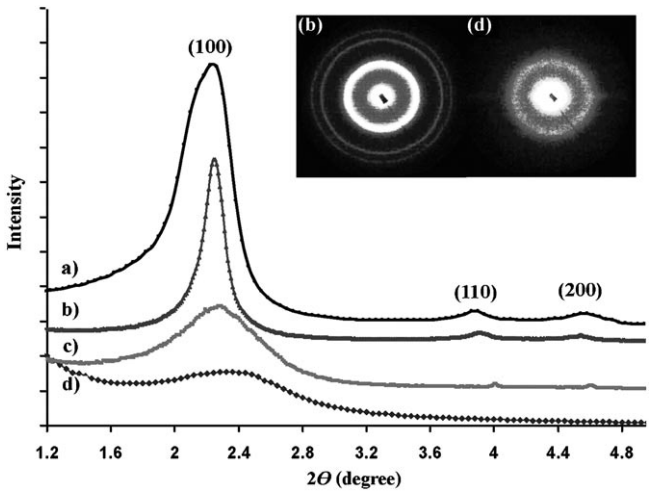

Figure 3. XRD patterns of electroactive PMOs with various compositions of TSUPQD and TEOS. a) 0 wt%; b) 5 wt%; c) 33 wt%; d) 66 wt%. Insets: Debye–Scherrer diffraction pattern rings of 5 wt% and 66 wt% TSU-PMOs, b and d, respectively.

Table 2. Structure and pore parameters of the PMOs after removal of templates.[a]

Sample [wt%]	d_{100} [nm]	a_o [nm]	S_{BET} [$m^2 g^{-1}$]	P_{BET} [nm]	P_{BJH} [nm]	W [nm]	V_{TOTAL} [$cm^3 g^{-1}$]
0	4.0	4.6	940	3.3	2.8	1.8	0.8
5	4.0	4.6	1054	3.5	2.8	1.8	0.9
20	3.9	4.5	844	2.5	2.5	2.0	0.5
33	3.9	4.5	423	2.3	2.2	2.3	0.2
66	3.8	4.4	190	2.8	2.1	2.4	0.1
66 nonporous	N/A	N/A	10	N/A	N/A	N/A	0.03

[a] a_o, the unit cell; S_{BET}, the BET specific surface area; P_{BET}, average mesopore diameter; P_{BJH}, dominate pore diameter (defined as peak value in the BJH pore size distribution curves for the pores diameters between 17 and 3000 Å in Figure S4 in the Supporting Information); W, wall thickness; V_{TOTAL}, total pore volume obtained from $P/P_0 = 0.99$.

Because the incorporated TSU bridges are not as mechanically strong as the continuous −Si−O− units, TSU-PMOs show deteriorated structural regularity and mesostructral features compared to pure silica matrix. To examine the influence of the TSU groups on interior pore parameters, nitrogen sorption characterization was conducted. Figure 4

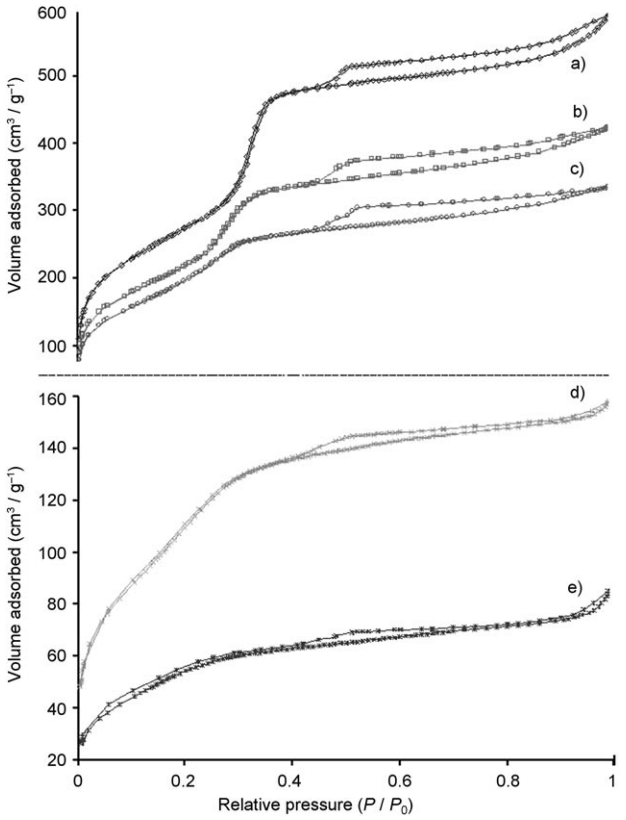

Figure 4. Nitrogen adsorption–desorption isotherms. a) 5 wt % TSU-PMO; b) 10 wt %; c) 20 wt %; d) 33 wt %; e) 66 wt %.

shows the nitrogen adsorption-desorption isotherms at −196 °C for TSU-PMOs with different TSU contents. In Figure 4, all of the nitrogen adsorption-desorption isotherms exhibit reversible capillary condensation/evaporation (type IV) behavior, characteristic of mesoporous materials.[31] Figure 4 and Figure S4 (see Supporting Information)together illustrate that the lower the TSU content, the steeper the capillary condensation branch (at $P/P_0 \approx 0.2$–0.3), and the more uniform the pore size in the material matrix. Also, the position of the capillary condensation branch shifts towards lower relative pressure with increasing concentration of TSU units, indicating smaller pore sizes in TSU-PMOs. All of the sorption isotherms show pronounced H4 type hysteresis loops[32] at relative pressures between about 0.99 and 0.45. This arises from the delayed capillary evaporation from secondary mesopores in mesoporous structures formed from filling the interparticle spaces.[33]

Table 2 lists the Brunauer–Emmett–Teller (BET) specific surface areas,[29] single-point adsorption total pore volumes,[30] and mesopore diameters for different TSU-PMO samples. Whereas the TSU content increases from 5 wt % to 66 wt %, the average mean pore diameters given from BJH distribution curves gradually shift from 2.8 nm to 2.1 nm, still within the range of mesopores. Meanwhile, the wall thickness increases from 1.8 nm to 2.4 nm. The trend of mesopore shrinkage with increasing TSU loading is also demonstrated by changes in the BET surface area and total pore volume, which indicate deteriorated mesostructural features with higher loading of TSU groups. These data from nitrogen sorption characterization are in agreement with the observation form XRD studies that 66 wt % TSU-PMO shows a structure with lower mesopore ordering.

Transmission electron microscopic (TEM) images of TSU-PMOs show ordered mesoporous structures with uniformly distributed hexagonal two-dimensional symmetry (Figure 5).

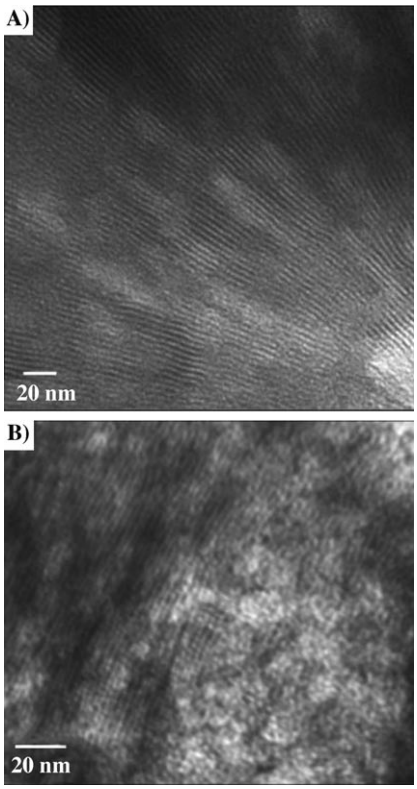

Figure 5. TEM images of oligoaniline-containing hybrid mesoporous organosilia: A) 20 wt % and B) 66 wt %. (scale bar: 20 nm).

But different amounts of TSU content give the images different features. For example, in the TEM images of 20 wt % TSU-PMO (Figure 5 A), evenly separated parallel fringes are clearly seen with mesopores aligned along the fringe extending axis, while in the images of 66 wt % TSU-PMO (Figure 5B), a deteriorated hexagonally patterned mesostructure is observed, demonstrating a less-ordered phase. However, both images are significantly different from that of the 100 wt % TSU-containing organosilica, which exhibits a disordered worm-like structure (see Figure S8 in the Supporting Information). The TEM images confirm that the mesoporous hexagonal pattern is maintained with up to 66 wt % of TSU moiety, while increasing the amount of incorporated TSU groups leads to reducing pore size (from 2.5 nm for 20 wt % TSU-PMO to 2 nm for 66 wt % TSU-PMO), which is consistent with the BJH calculation and XRD studies.

As reported before,[23] the precursor TSUPQD showed essentially similar electrochemical behavior as polyaniline but with slightly higher redox peak potentials which are attribut-

ed to the electron withdrawing ureido groups attached to the main chain of the amino-capped aniline trimer (see Figure S5 in the Supporting Information). Based on this phenomenon, we studied the electrochemical behavior of TSU-PMOs in both aqueous and non-aqueous solutions. Cyclic voltammograms (CVs) obtained in strongly acidic aqueous solutions of HCl (1 M) for TSU-PMOs with different TSU content are shown in Figure 6. Because the ana-

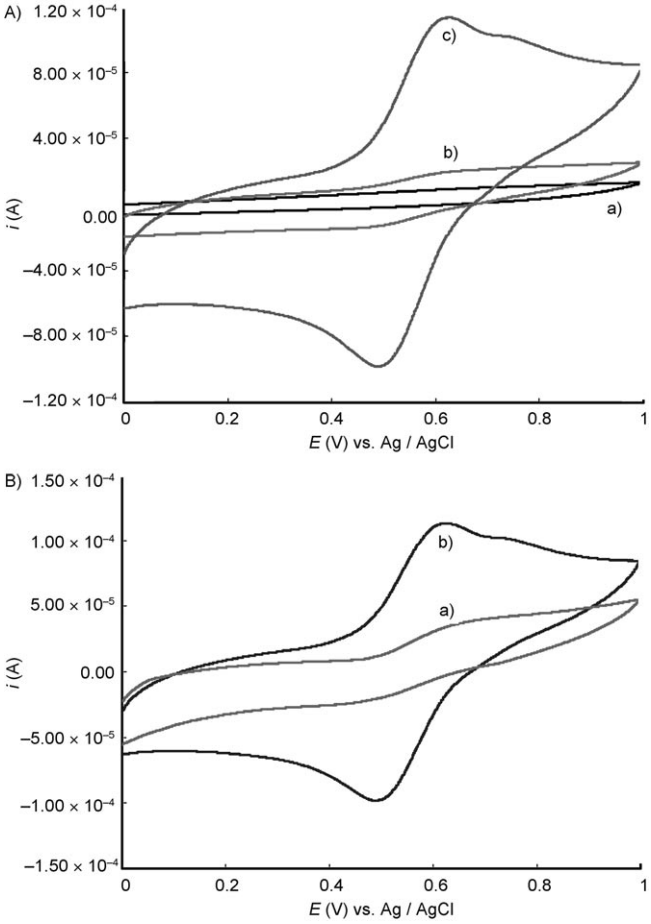

Figure 6. A) Cyclic voltammograms of a) 0 wt%, b) 33 wt%, and c) 66 wt% TSU-PMO in aqueous solution of HCl. B) Cyclic voltammograms of a) 66 wt% nonporous TSU-organosilica and b) 66 wt% TSU-PMO.

lytes are insoluble in aqueous conditions, the samples were wrapped in platinum foil electrodes for measurements. In the scanned potential range shown (0–1.0 V), one well defined redox pair of peaks was found at around 0.55 V against the reference electrode (Ag/AgCl) which corresponds to the transition from the "leucoemeraldine" to the "emeraldine" form of the aniline oligomer and represents the removal/addition of two electrons.[34] The second redox pair of peaks which corresponds to the oxidation of the "emeraldine" form to the "pernigraniline" form cannot be detected in aqueous solution due to the background range limit from water. To observe this redox pair of peaks, measurements were conducted in non-aqueous solutions. Figure 7 shows

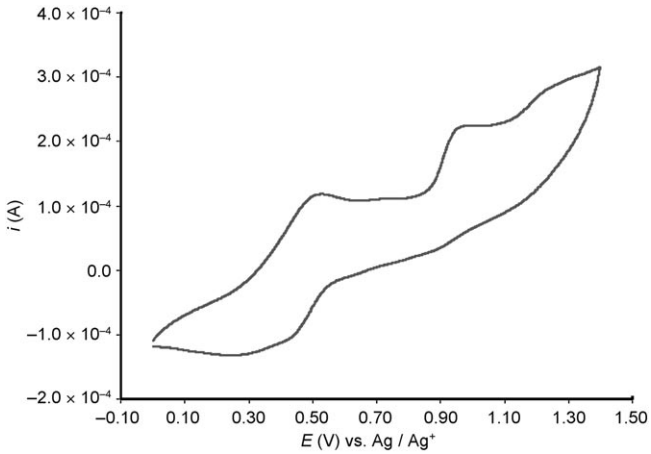

Figure 7. Cyclic voltammogram of the electroactive hybrid made from 100 wt% TSUPQD.

the CV obtained in acetonitrile for the electroactive hybrid made from 100 wt% of TSUPQD, which clearly shows two pairs of redox peaks. However, CVs of TSU-PMOs in nonaqueous solutions do not give as obvious redox peaks as in water due to the inadequate interactions between TSU-PMOs and organic dopants or electrolytes. So, electrochemical studies of TSU-PMOs in aqueous conditions were chosen and the redox pair of peaks corresponding to the transition from the "leucoemeraldine" to the "emeraldine" form was used to compare the electroactivities for different TSU-PMO materials.

The cyclic voltammograms indicate that the electroactivity from the electroactive aniline trimer moiety is maintained in TSU-PMOs. However, substantially lower intensities of the redox peaks for TSU-PMOs were observed compared to the electroactive precursor (TSUPQD) under the same conditions, which are caused by co-condensation with electrochemically inert TEOS and the formation of a rigid inorganic silica framework. It is not surprising that the introduced electroactive function can be well controlled by adjusting the content of oligoaniline bridges in the organosilica. As seen in Figure 6A, 66 wt% TSU-PMO shows more than one order of magnitude higher currents than lower content (33 wt%) TSU-PMOs, which is consistent with the fact that 66 wt% TSU-PMO has more redox sites than lower content TSU-PMOs.

The electrochemical activity of these redox sites was established by direct electron transfer from the working electrode surface to the electroactive sites[35] and/or through long range electron transfer through electron exchange between the adjacent electroactive moieties (electron hopping).[19,36] It is worth noting that the electrochemical behavior of the mesoporous 66 wt% TSU-PMO is significantly different from that of the nonporous 66 wt% TSU-contained organosilica as depicted in Figure 6B. This may be attributed to the fact that the uniform mesopores provide more rapid electrolyte diffusions, and enhanced ordering of adjacent electroactive groups facilitates the electron exchange between the active redox centers and the working

electrode. From this electrochemical study, it can be stated that the MCM-41 mesoporous structure not only retains the anticipated electroactivity for this series of hybrid materials but even enhances the electrochemical performance compared to conventional bulk materials. The conductivity measurement result ($\approx 10^{-5}\,S\,cm^{-1}$) for HCl-doped 66 wt% TSU-PMO using a four-probe method is also in good accordance with this statement. Compared to the aniline trimer though, this measurement shows a two orders of magnitude decrease in conductivity, which arises from the presence of the non-conducting inorganic silica matrix.

The chemical accessibility of TSU-PMOs was evaluated by examining their uptake of an organic dopant, 10-camphorsulfonic acid (HCSA), and the results were compared to their nonporous counterparts, nonporous TSU-silica (Figure 8). When treated with HCSA, the electroactive oligoaniline groups in both hybrid materials were converted from an emeraldine base to an emeraldine salt, with H^+ doped aniline trimer as the cation and CSA^- as the anion. The uptake of HCSA caused a weight increase for both materials. In the case of pure silica matrix, the periodic mesoporous silica (0 wt% TSU-PMO) showed nearly no mass uptake compared to nonporous silica, which indicates that simple mesopores are not good reservoirs for HCSA. In fact, the electrostatic attraction between cationic oligoaniline units and anionic CSA^- groups is the driving force for HCSA uptake. As shown in Figure 8, a higher content of oligoaniline units in TSU-PMOs leads to a larger weight increase, which confirms that the electrostatic interaction is the dominating factor (more so than the surface adsorption) to control the mass uptake of HCSA. For example, 33 wt% TSU-PMO which showed a smaller surface area than the 5 wt% TSU-PMO gave a mass increase of a (25.18 ± 0.42) wt%, whereas 5 wt% TSU-PMO only gave a mass increase of (7.47 ± 0.19) wt%. However, pore parameters are still important factors effecting chemical accessibility. TSU-PMOs always showed considerably higher weight increase over the nonporous TSU-silica. For example, 10 wt% TSU-PMO gained (13.28 ± 0.13) wt% after HCSA doping, whereas nonporous 10 wt% TSU-silica gained only (5.30 ± 0.10) wt% and both weight increases are below the theoretical value of 17.82 wt% calculated from the amount of TSUPQD precursor used in the material fabrication process. These results clearly illustrate that not all of the oligoaniline trimer units in the hybrid materials are accessible to bulky camphorsulfonate groups, larger surface areas, and more interior channels make the organic moiety in TSU-PMOs more accessible for further functionalizations.

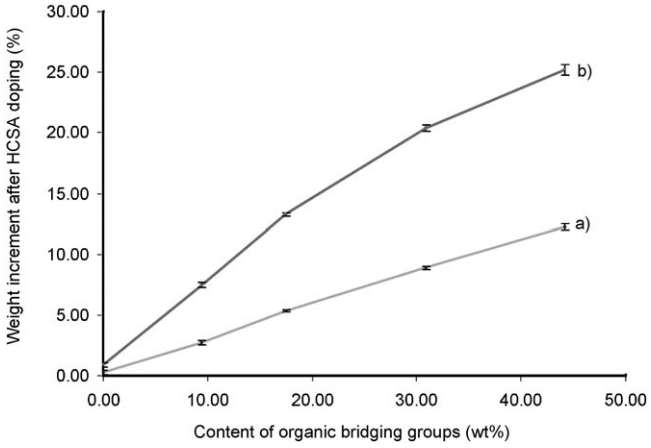

Figure 8. Mass uptake of L-camphorsulfonate for a) nonporous organosilica and b) mesoporous TSU-PMOs.

Conclusion

We have developed a novel group of electroactive PMOs as the analogue of the electrically conductive polymer-polyaniline using a surfactant CTAB-templated approach. The resultant PMOs maintain hexagonally patterned mesostructures with TSUPQD loading of up to 66 wt% and mesopore diameters in the range of 2–3 nm. The integrated oligoaniline components show direct effects on interior surface area, uniformity of pore diameters, and channel twisting. With slightly deteriorated mesoporous structural properties, the TSU-PMOs with higher contents of oligoaniline moiety exhibit enhanced electroactivity over TSU-PMOs with lower oligoaniline loadings. The introduction of unique electroactivity with retention of the mesoporous reservoirs makes this series of hybrid materials promising in manufacturing electrochemically switchable devices. Further work on applying them as tunable host-guest systems for protein delivery is in progress. The synthetic strategy employed in this study may also be applied to other "synthetic metals"[37] to introduce a variety of physiochemical properties into an inorganic silica matrix.

Experimental Section

Materials and synthesis: The emeraldine base aniline trimer *N,N′*-bis(4′-aminophenyl)-1,4-quinonene-diimine (EBAT) was prepared following the established procedure developed in our group[24] and was purified by Soxhlet extraction with acetone. Triethoxysilylpropyl isocyanate (TESPIC), tetraethyl orthosilicate (TEOS), cetyltrimethylammonium bromide (CTAB), L-10-camphorsulfonic acid (HCSA), ammonium hydroxide (29.82 wt% $NH_3{\cdot}H_2O$), and acetone (reagent grade) were purchased from Sigma-Aldrich and used as received.

The silsesquioxane precursor *N,N′*-bis(4′-(3-triethoxysilylpropylureido)-phenyl)-1,4-quinonenediimine (TSUPQD) was prepared from the one-step reaction between *N,N′*-bis(4′-aminophenyl)-1,4-quinonene-diimine (EBAT) and triethoxysilylpropyl isocyanate (TESPIC) at a molar ratio of 1:2 in THF followed by addition of an excessive amount of *n*-hexane to precipitate the product as a wine-red solid.[23]

A typical procedure for synthesizing electroactive PMOs (66 wt% TSUPQD) is as follows. Cetyltrimethylammonium bromide (CTAB, 129.7 mg, 0.36 mmol) was dissolved in 16 wt% $NH_3{\cdot}H_2O$ (5.82 g, 54.8 mmol), and the solution was stirred at 40 °C in a sealed polyethylene bottle for 1 hour. After cooling to room temperature, TEOS (80 mg, 0.38 mmol) were added to the solution and the mixture was stirred until a homogenous solution was obtained, indicating the complete hydrolysis of TEOS. To this solution, TSUPQD (160 mg, 0.21 mmol) in acetone

(2 mL) was added, and the resulted mixture was stirred at 50 °C for 12 h, followed by aging at 100 °C for 1 day. The mixture was then cooled to room temperature, the resultant black solid was filtered off and air dried overnight.

To obtain TSU-PMOs with varying amount of aniline trimer contents, different weight ratios of TSUPQD and TEOS were used in the procedure as summarized in Table 1. To ensure that the pore parameters of TSU-PMOs are affected only by the amount of TSUPQD instead of changes in the surfactant or the solvent, all of the PMO samples studied were prepared with the same amounts of CTAB, ammonia, and acetone. As a control, non-porous TSU organosilica was also prepared under the same conditions, except for the absence of the surfactant CTAB.

Postsynthesis treatment: The surfactant molecules were removed by extracting the solid for 12 h using a mixture of ethanol (25 mL), 2 M HCl (2 mL), and *n*-hexane (1 mL) for all of the materials prepared as described above. Weight losses of about 10–50 % were found after thorough extraction. For convenience throughout this article, TSU-PMOs are labeled with their loading percentage of TSUPQD. For instance, 20 wt % TSU-PMO defines the organosilica prepared from co-condensation of 20 wt % TSUPQD and 80 wt % TEOS. To evaluate the chemical accessibility of aniline trimer moieties, each emeraldine base of a PMO sample (50 mg) was added to 5 wt % organic dopant L-10-camphorsulfonic acid (HCSA, 10 mL) in aqueous solution and ultra-sonicated for 1 hour. The solid was filtered, washed with deionized water and dried under vacuum at 50 °C for 24 h. The weight gained after the treatment was attributed to the CSA^- attached to the doped TSU-PMOs by electrostatic interaction.

Characterization: Infrared (IR) spectra were recorded as KBr pellets with a Perkin Elmer 1600 Fourier transform infrared spectrometer (FT-IR). Studies of thermal properties were taken on a TA Instruments Thermogravimetric analyzer Q50 at a heating rate of 20 K/min under static air conditions. The structure of the mesoporous organosilica materials was characterized by small-angle X-ray diffraction (XRD), recorded on a Gerrman Bruker multi-angle X-ray diffractometer with $Cu_{K\alpha}$ radiation (40 KV, 85 mA). Transmission electron microscopic (TEM) images were obtained with a Hitachi 7600 Transmission Electron Microscope. Nitrogen adsorption/desorption isotherms, pore size distributions, and textural properties of the materials were measured using a Micromeritics ASAP 2000 system. Before N_2 adsorption/desorption analysis, the samples were evacuated and dried at 100 °C for 12 h. The BET surface area was calculated from adsorption data in the relative pressure range from 0.01 to 0.3. Electrochemical measurements were performed using an Epsilon Potensiostat (Bioanalytical Systems, Inc.) interfaced with a PC computer. A three-electrode system was employed, consisting of a platinum foil electrode with a surface area of 0.25 cm^2, a platinum-wire auxiliary electrode and a reference electrode. The reference electrodes used were Ag/AgCl for aqueous solutions and Ag/Ag^+ (silver ions as 0.01 M $AgNO_3$ in a solution of MeCN containing 0.1 M Et_4NPF_6) for nonaqueous solutions. Electric conductivity measurements were performed with a 4-probe device (PAR Model 173 Potentiostat/Galvanostat).

Acknowledgements

This work was supported in part by the US Army Research Office (ARO), National Institutes of Health (NIH No. DE09848) and the Nanotechnology Institute of Southeastern Pennsylvania. The authors are very grateful to Prof. Norman R. Dollahon and Ms. Sally R. Shrom (Villanova University, PA 19085) for their kind assistance with the TEM measurements.

[1] C. T. Kresge, M. E. Leonowicz, W. J. Roth, J. C. Vartuli, J. S. Beck, *Nature* **1992**, *359*, 710–712.

[2] a) K. J. Shea, D. A. Loy, *Chem. Mater.* **1989**, *1*, 572–574; b) D. A. Loy, K. J. Shea, *Chem. Rev.* **1995**, *95*, 1431–1442; c) R. J. P. Corriu, D. Leclercq, *Angew. Chem.* **1996**, *108*, 1524–1540; *Angew. Chem. Int. Ed.* **1996**, *35*, 1420–1436; d) R. J. P. Corriu, *Angew. Chem.* **2000**, *112*, 1432–1455; *Angew. Chem. Int. Ed.* **2000**, *39*, 1376–1398.

[3] a) T. Asefa, M. J. MacLachlan, N. Coombs, G. A. Ozin, *Nature* **1999**, *402*, 867–871; b) S. Inagaki, S. Guan, Y. Fukushima, T. Ohsuna, O. Terasaki, *J. Am. Chem. Soc.* **1999**, *121*, 9611–9614; c) B. J. Melde, B. T. Holland, C. F. Blanford, A. Stein, *Chem. Mater.* **1999**, *11*, 3302–3308; d) C. Yoshina-Ishii, T. Asefa, N. Coombs, M. J. MacLachlan, G. A. Ozin, *Chem. Commun.* **1999**, *24*, 2539–2540; e) A. Stein, B. J. Melde, R. C. Schroden, *Adv. Mater.* **2000**, *12*, 1403–1419.

[4] R. H. Baney, M. Itoh, A. Sakakibara, T. Suzuki, *Chem. Rev.* **1995**, *95*, 1409–1430.

[5] a) E. Cho, K. Kwon, K. Char, *Chem. Mater.* **2001**, *13*, 3837–3839; b) E. Cho, K. Char, *Chem. Mater.* **2004**, *16*, 270–275; c) H. Zhu, D. J. Jones, J. Zajac, J. Roziere, R. Dutartre, *Chem. Commun.* **2001**, *24*, 2568–2569; d) O. Muth, C. Schellbach, M. Froeba, *Chem. Commun.* **2001**, *19*, 2032–2033; e) J. R. Matos, M. Kruk, L. P. Mercuri, M. Jaroniec, T. Asefa, N. Coombs, G. A. Ozin, T. Kamiyama, O. Terasaki, *Chem. Mater.* **2002**, *14*, 1903–1905; f) M. C. Burleigh, M. A. Markowitz, E. M. Wong, J. Lin, B. Gaber, *Chem. Mater.* **2001**, *13*, 4411–4412.

[6] a) F. Hoffmann, M. Cornelius, J. Morell, M. Froeba, *Angew. Chem.* **2006**, *118*, 3290–3328; *Angew. Chem. Int. Ed.* **2006**, *45*, 3216–3251; b) Y. Lu, H. Fan, N. Doke, D. A. Loy, R. A. Assink, D. A. LaVan, C. J. Brinker, *J. Am. Chem. Soc.* **2000**, *122*, 5258–5661; c) V. Y. Gusev, X. Feng, Z. Bu, G. L. Haller, J. O' Brien, *J. Phys. Chem.* **1996**, *100*, 1985–1988.

[7] M. C. Burleigh, M. A. Markowitz, S. Jayasundera, M. S. Spector, C. W. Thomas, B. P. Gaber, *J. Phys. Chem. B* **2003**, *107*, 12628–12634.

[8] Q. Yang, M. P. Kapoor, S. Inagaki, N. Shirokura, J. N. Kondo, K. Domen, *J. Mol. Catal. A: Chem.* **2005**, *230*, 85–89.

[9] Y. P. He, S. Q. Wang, C. R. Li, Y. M. Miao, Z. Y. Wu, B. S. Zou, *J. Phys. D: Appl. Phys.* **2005**, *38*, 1342–1350.

[10] H. Jeong, C. Kwak, C. Ha, S. Seul, *Mol. Cryst. Liq. Cryst. Sci. Technol. Sect. A* **2004**, *425*, 173–180.

[11] a) Q. Huo, D. I. Margolese, U. Ciesla, P. Feng, T. E. Gier, P. Sieger, R. Leon, P. M. Petroff, F. Schueth, G. D. Stucky, *Nature* **1994**, *368*, 317–321; b) W. J. Hunks, G. A. Ozin, *J. Mater. Chem.* **2005**, *15*, 3716–3724.

[12] a) T. Asefa, M. J. MacLachlan, H. Grondey, N. Coombs, G. A. Ozin, *Angew. Chem.* **2000**, *112*, 1878–1881; *Angew. Chem. Int. Ed.* **2000**, *39*, 1808–1811; b) D. Gray, S. Hu, E. Juang, D. Gin, *Adv. Mater.* **1997**, *9*, 731–736; c) A. Sayari, S. Hamoudi, *Chem. Mater.* **2001**, *13*, 3151–3168; d) S. Inagaki, S. Guan, T. Ohsuna, O. Terasaki, *Nature* **2002**, *416*, 304–307; e) M. P. Kapoor, Q. Yang, S. Inagaki, *J. Am. Chem. Soc.* **2002**, *124*, 15176–15177; f) H. Furukawa, M. Hibino, H. Zhou, I. Honma, *Chem. Lett.* **2003**, *32*, 132–133.

[13] D. R. Rolison, *Science* **2003**, *299*, 1698–1702.

[14] P. Audebert, C. J. Sanchez, *J. Sol-Gel Sci. Technol.* **1994**, *2*, 809–812.

[15] a) W. J. Hunks, G. A. Ozin, *Adv. Funct. Mater.* **2005**, *15*, 259–266; b) K. Landskron, B. D. Hatton, D. D. Perovic, G. A. Ozin, *Science* **2003**, *302*, 266–269; c) R. J. P. Corriu, A. Mehdi, C. Reye, C. Thieuleux, *Chem. Commun.* **2002**, *13*, 1382–1383.

[16] M. Kuroki, T. Asefa, W. Whitnal, M. Kruk, C. Yoshina-Ishii, M. Jaroniec, G. A. Ozin, *J. Am. Chem. Soc.* **2002**, *124*, 13886–13895.

[17] J. Liu, J. Yang, Q. Yang, G. Wang, Y. Li, *Adv. Funct. Mater.* **2005**, *15*, 1297–1302.

[18] R. M. Grudzien, B. E. Grabicka, S. Pikus, M. Jaroniec, *Chem. Mater.* **2006**, *18*, 1722–1725.

[19] D. F. Rohlfing, J. Rathousky, Y. Rohlfing, O. Bartels, M. Wark, *Langmuir* **2005**, *21*, 11320–11329.

[20] C. Delacote, J. Bouillon, A. Walcarius, *Electrochim. Acta* **2006**, *51*, 6373–6383.

[21] Y. Bai, H. Yang, W. Yang, Y. Li, C. Sun, *Sens. Actuators, B* **2007**, *124*, 179–186.

[22] a) A. G. MacDiarmid, *Angew. Chem.* **2001**, *113*, 2649–2659; *Angew. Chem. Int. Ed.* **2001**, *40*, 2581–2590; b) H. He, J. Zhu, N. Tao, J. Nagahara, I. Amlani, R. Tsui, *J. Am. Chem. Soc.* **2001**, *123*, 7730–7731; c) J. Huang, R. B. Kaner, *J. Am. Chem. Soc.* **2004**, *126*, 851–855.

[23] Y. Guo, A. Mylonakis, Z. Zhang, P. I. Lelkes, K. Levon, S. Li, Q. Feng, Y. Wei, *Macromolecules* **2007**, *40*, 2721–2729.
[24] Y. Wei, C. Yang, T. Ding, *Tetrahedron Lett.* **1996**, *37*, 731–734.
[25] H.-P. Lin, C.-Y. Mou, *Acc. Chem. Res.* **2002**, *35*, 927–935.
[26] M. Angelopoulos, A. Ray, A. G. MacDiarmid, A. J. Epstein, *Synth. Met.* **1987**, *21*, 21–30.
[27] a) S. Quillard, G. Louarn, S. Lefrant, A. G. MacDiarmid, *Phys. Rev. B* **1994**, *50*, 12496–12508; b) I. Harada, Y. Furukawa, F. Ueda, *Synth. Met.* **1989**, *29*, E303-E312; c) Y. Furukawa, F. Ueda, Y. Hyodo, I. Harada, T. Nakajima, T. Kawagoe, *Macromolecules* **1988**, *21*, 1297–1305.
[28] O. Olkhovyk, S. Pikus, M. Jaroniec, *J. Mater. Chem.* **2005**, *15*, 1517–1519.
[29] S. Brunauer, P. H. Emmett, E. Teller, *J. Am. Chem. Soc.* **1938**, *60*, 309–319.
[30] K. S. W. Sing, D. H. Everett, R. A. W. Haul, L. Moscou, R. A. Pierotti, J. Rouquerol, T. Siemieniewska, *Pure Appl. Chem.* **1985**, *57*, 603–619.
[31] IUPAC Manual of Symbols and Terminology, Appendix 2, Part 1, *Pure Appl. Chem.* **1972**, *31*, 578.
[32] E. C. Donaldson, N. Ewall, B. Singh, *J. Pet. Technol.* **1991**, *6*, 249–261.
[33] J. R. Matos, L. P. Mercuri, M. Kruk, M. Jaroniec, *Langmuir* **2002**, *18*, 884–890.
[34] a) Y. Wei, Y. Sun, X. Tang, *J. Phys. Chem.* **1989**, *93*, 4878–4881; b) N. Yamada, R. B. Kaner, E. Chang, *Plast. Eng.* **1998**, *45*, 763–821.
[35] a) M. Endo, Y. J. Kim, K. Osawa, K. Ishii, T. Inoue, T. Nomura, N. Miyashita, M. S. Dresselhaus, *Electrochem. Solid-State Lett.* **2003**, *6*, A23A26; b) Y. Yamauchi, T. Momma, H. Kitoh, T. Osaka, K. Kuroda, *Electrochem. Commun.* **2005**, *7*, 1364–1370.
[36] a) G. Inzelt, *Chem. Biochem. Eng. Q.* **2007**, *21*, 1–14; b) A. Domenech, M. Alvaro, B. Ferrer, H. Garcia, *J. Phys. Chem. B* **2003**, *107*, 12781–12788.
[37] A. J. Heeger, *Synth. Met.* **2001**, *125*, 23–42.

Received: October 11, 2007
Published online: January 25, 2008

